Available online at www.sciencedirect.com
SCIENCE DIRECT®
Journal of Molecular Spectroscopy 237 (2006) 63–69
Journal of MOLECULAR SPECTROSCOPY
www.elsevier.com/locate/jms

Cavity ring-down spectroscopy of $H_2{}^{17}O$ in the range 16 570–17 125 cm^{-1}

O. Naumenko [a], M. Sneep [b], M. Tanaka [c], S.V. Shirin [d], W. Ubachs [b,*], J. Tennyson [c]

[a] Russian Academy of Science, Institute of Atmospheric Optics, Tomsk, 634055, Russia
[b] Laser Centre, Department of Physics and Astronomy, Vrije Universiteit, De Boelelaan 1081, 1081 HV Amsterdam, The Netherlands
[c] Department of Physics and Astronomy, University College London, London WC1E 6BT, UK
[d] Russian Academy of Science, Institute of Applied Physics, Nizhnii Novgorod 603950, Russia

Received 21 September 2004; in revised form 16 February 2006
Available online 29 March 2006

Abstract

Following previous investigations on $H_2{}^{16}O$ and $H_2{}^{18}O$ by cavity ring-down spectroscopy, this method has now been applied to investigate the energy region of the 5*v* polyad in the absorption spectrum of $H_2{}^{17}O$. In the range 16 570–17 125 cm^{-1}, the highest energy range investigated for the $H_2{}^{17}O$ isotopologue so far, 516 lines are attributed to $H_2{}^{17}O$ and assigned from a newly generated line list.

PACS: 33.20.Kf; 33.15.Mt; 92.60.Jq

Keywords: Water vapor; Visible spectra; Isotopologues; Cavity ring-down; Water vapor spectrum; Atmosphere

1. Introduction

The absorption spectrum of water vapor in the 16 570–17 125 cm^{-1} energy range covers the entire 5*v* polyad, which lies in a window used for remote sensing of this molecule, which is considered the most important greenhouse gas. Retrieval of water vapor column densities, using this rather weak absorption feature on a global scale has been demonstrated with data obtained by the satellite instrument SCIAMACHY [1,2]. Naus et al. [3] studied the absorption spectrum of natural water (containing 99.732% $H_2{}^{16}O$, 0.200% $H_2{}^{18}O$, 0.037% $H_2{}^{17}O$, and 0.031% HDO, see also [4]) in the frequency region 16 555–18 000 cm^{-1} employing the laser-based technique of cavity ring-down (CRD) spectroscopy. Due to the good signal-to-noise ratio provided by the highly sensitive CRD method 1830 lines were found of which 800 were not included in HITRAN 96, the database prevailing at the time. Of the set of weak lines 111 were given an assignment from a comparison with first principles calculations. Subsequently from a ^{18}O isotopically enriched water sample a narrower energy region, still covering the most intense part of the 5*v* polyad, was investigated for $H_2{}^{18}O$, yielding 596 lines belonging to $H_2{}^{18}O$, of which 375 could be assigned based on the production of a new theoretical line list [5]. Here, in a continuation of this work, we report of an investigation of the $H_2{}^{17}O$ spectrum, again covering the 5*v* polyad, using the same CRD setup at the Laser Centre VU Amsterdam. From a comparison with spectra of $H_2{}^{16}O$ and $H_2{}^{18}O$ 516 lines are attributed to $H_2{}^{17}O$ and assigned on the basis of a newly produced line list. After previous investigations in the mid-infrared reporting on $H_2{}^{17}O$ (000) and (010) rotational states [6], overtone rovibrational transitions were investigated in the energy regions 6600–7640 cm^{-1} [7], 9711–11 335 cm^{-1} [8], and 11 335–14 520 cm^{-1} [9]. The present observations are in the highest energy region investigated so far for $H_2{}^{17}O$.

2. Experimental

The experimental procedures and conditions are very similar to the ones used for the $H_2{}^{16}O$ and $H_2{}^{18}O$ measurements

* Corresponding author.
E-mail address: wimu@nat.vu.nl (W. Ubachs).

0022-2852/$ - see front matter © 2006 Elsevier Inc. All rights reserved.
doi:10.1016/j.jms.2006.02.012

described previously [3,5]. In short, a cavity ring-down experiment was performed using a cell of length ≈85 cm sealed with mirrors of reflectivity ≈99.99% and radius of curvature of 50 cm. Tunable laser radiation in pulses of 5 ns and bandwidth ≈0.06 cm^{-1}, obtained from a Nd:YAG pumped dye laser system (Quanta-Ray PDL-3), was employed to induce the ring-down transients. The observed exponential decays were converted into an absorption spectrum following well-established methods [10]. In case of very strong lines the obtained decay transients are almost fully collapsed, causing saturation in the absorption profiles. Line positions and intensities were obtained from the resulting absorption spectrum by fitting Voigt profiles to the resonances.

Isotopic composition of the ^{17}O-enriched water sample (CAMPRO Scientific) was: 83.8% atom ^{17}O, 8.3% atom ^{16}O, and 7.9% atom ^{18}O. The contamination of $H_2{}^{16}O$ was estimated to be about 10% and that of $H_2{}^{18}O$ is roughly the same because of the residuals from the sample cell and mirrors, which were used for the previous $H_2{}^{18}O$ measurements. This leaves about 80% of sample water belonging to $H_2{}^{17}O$, with an estimated error of about 5%. The total pressure during the measurements was at the saturation point of water at 294 ± 1 K, corresponding to 25 mbar. As for the frequency positions the $H_2{}^{17}O$ lines were calibrated against an I_2 reference spectrum [11] as well as against the known line positions of $H_2{}^{16}O$ and $H_2{}^{18}O$ lines, resulting in an estimated accuracy of 0.05 cm^{-1}.

To eliminate the $H_2{}^{16}O$ and $H_2{}^{18}O$ lines and to identify the lines belonging to $H_2{}^{17}O$, the spectrum of natural abundance water vapor by Naus et al. [3] and the $H_2{}^{18}O$ spectrum by Tanaka et al. [5] were plotted with the $H_2{}^{17}O$ spectrum in a single graph. Fig. 1 shows a portion of the graph with the natural abundance (top), $H_2{}^{17}O$ (middle), and $H_2{}^{18}O$ spectrum (bottom). The $H_2{}^{16}O$ lines are narrower than the $H_2{}^{17}O$ and $H_2{}^{18}O$ lines because of the different pressure conditions used in the experiments. Each line in the $H_2{}^{17}O$ spectrum was manually attributed to $H_2{}^{16}O$, $H_2{}^{17}O$ or $H_2{}^{18}O$. After this procedure, 516 lines are

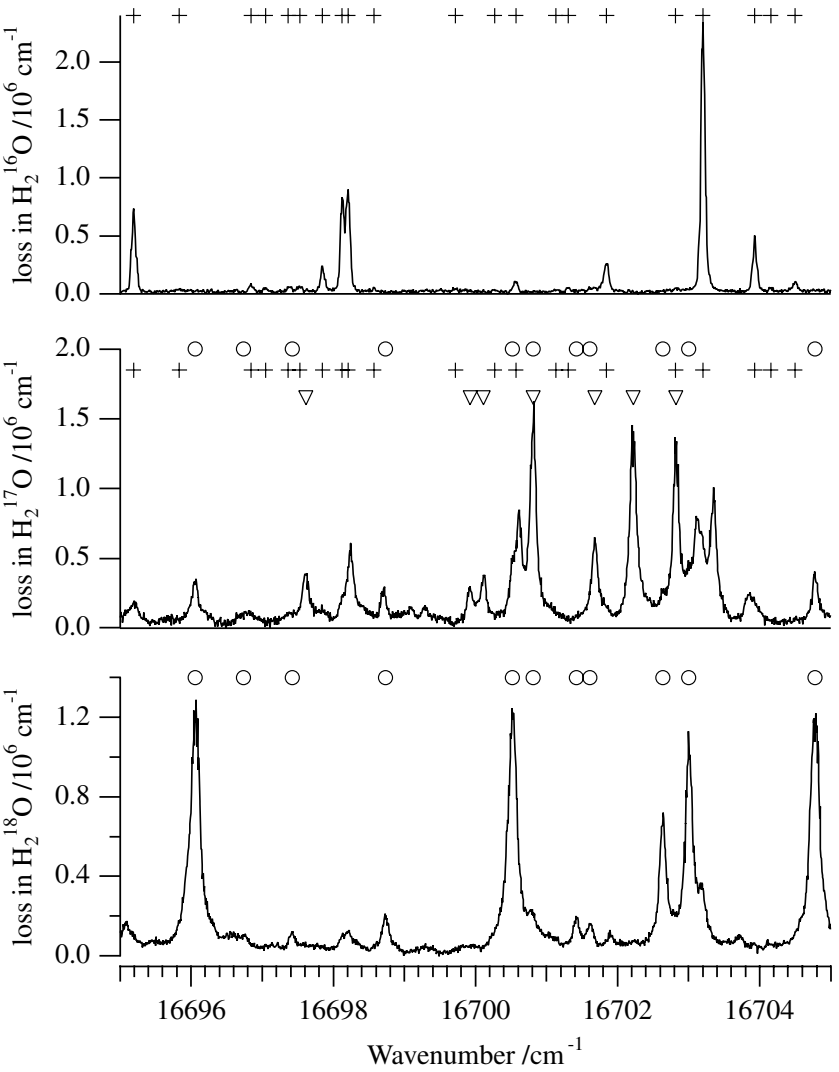

Fig. 1. A portion of the measured spectrum of $H_2{}^{17}O$ (middle) compared with natural abundance spectrum by Naus et al. [3] (top) and $H_2{}^{18}O$ spectrum by Tanaka et al. [5] (bottom). The markers indicate line positions of the different isotopologues—$H_2{}^{16}O$ (+), $H_2{}^{17}O$ (▽), and $H_2{}^{18}O$ (○).

identified as belonging to $H_2{}^{17}O$. Of these 516 lines, 32 and 27 lines are found to be overlapped by lines pertaining to $H_2{}^{16}O$ and $H_2{}^{18}O$, respectively. All lines attributed to $H_2{}^{17}O$ are presented in the Appendix to this paper, which is deposited in the electronic archive of the Journal of Molecular Spectroscopy. The resulting line list contains 576 transitions taking into account unresolved multiplets.

3. Assignment results

A theoretical line list for $H_2{}^{17}O$, at a temperature of 296 K, was calculated using the DVR3D program suite [12] with potential energy surfaces (PES) by Shirin et al. [13]. This adiabatic potential energy surface for three major isotopologues of water, $H_2{}^{16}O$, $H_2{}^{17}O$, and $H_2{}^{18}O$, was constructed by fitting to a large set of vibration–rotation energy levels of the three isotopologues known at the time. The fit was based on 1788 experimental energy levels with rotational quantum numbers $J = 0$, 2, and 5 and reproduced these observed levels with a standard deviation of 0.079 cm^{-1}.

Table 1
Summary of $H_2{}^{17}O$ vibrational energy levels determined in this study

Band	Origin (cm^{-1})	Number of levels	Number of transitions
(340) or 30^+4		14	19
(241) or 30^-4		9	10
(043) or 21^-4		5	9
(142) or 21^+4		16	19
(420) or 40^+2	16798.83 (10)	66	86
(321) or 40^-2	16797.167	71	135
(222) or 31^+2		1	1
(123) or 31^-2		2	2
(500) or 50^+0	16875.27 (2)	51	92
(401) or 50^-0	16875.620	61	135
(302) or 41^+0		2	1
(260) or 20^+6		3	5
(161) or 20^-6		1	1
(081) or 10^-8		1	1
	Total	303	516

Bands are labelled using normal mode (left) and local mode (right) notations. Number of levels shows the number of newly determined energy levels. Number of transitions shows the number of transitions to the vibrational bands.

This line list for $H_2{}^{17}O$ is built upon energy levels up to 26000 cm^{-1} and $J \leqslant 10$. The DVR3D [12] was used with 29 radial grid points for Morse oscillator-like basis functions and 40 angular grid points based on (associated) Legendre polynomials. Vibrational Hamiltonian matrices of final dimension 1500 were diagonalised and for rotational problems these matrices had dimension $300 \times (J + 1 - p)$, where J is the rotational quantum number and p, the parity. Nuclear masses of ^{17}O and H have been used to generate the line list. For the intensity calculations the best available dipole moment surface (DMS) of Schwenke and Partridge [14] was used.

Assignments were made relying on matches between observed and calculated frequencies and intensities. For this purpose values for absolute intensities (in cm molecule^{-1}) were estimated based on sample pressure and relative abundance of $H_2{}^{17}O$ in the gaseous sample. The intensities are put on an absolute scale for $H_2{}^{17}O$ in natural abundance by adopting 0.0372% of $H_2{}^{17}O$, normalizing to 296 K as in HITRAN [15] and using partition functions $Q(294) = 1037.253$ and $Q(296) = 1047.931$ (from cfa-ftp.harvard.edu). The uncertainties in the line intensities, listed in the Appendix, are at least 15% for medium intensity and well isolated lines, and may be significantly larger for the weakest lines. This uncertainty also includes an

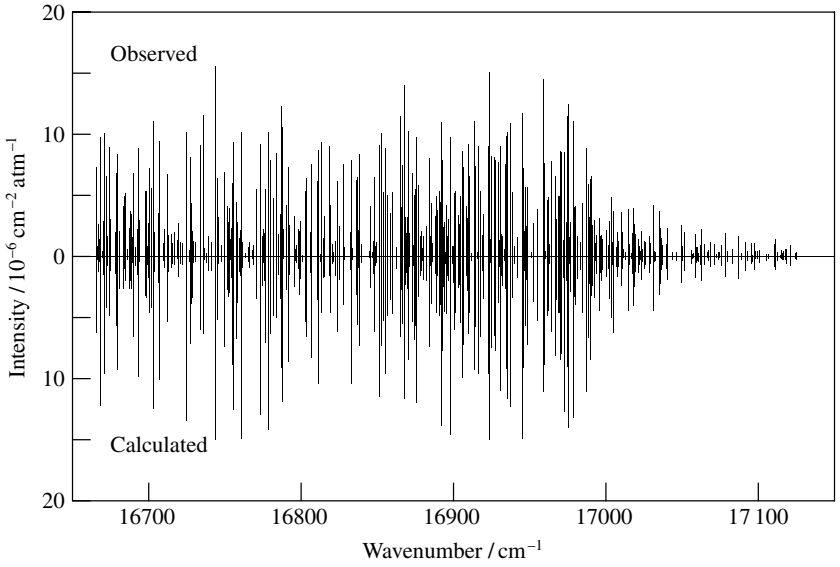

Fig. 2. Overview of the $H_2{}^{17}O$ experimental spectrum and the calculated line list in the 5v polyad region. For making a good comparison the experimental line positions and derived intensities are converted into a stick spectrum. Only 451 weakest lines of 516 observed are included in the comparison (see text). The intensities of the experimental spectrum are not scaled to its natural abundance as is common in the HITRAN database; we have chosen to present here the line strengths pertaining to the pure $H_2{}^{17}O$ isotopologue.

Table 2
$H_2{}^{17}O$ energy levels in cm^{-1} for the (321), (420), (500), and (401) vibrational states

J	K_a	K_c	(321)			(420)			(401)			(500)		
0	0	0	16797.167		1				16875.620		1			
1	0	1	16819.528		1				16897.698	19.1	2	16897.357		1
1	1	1	16834.715	7.3	2				16908.774	0.7	2	16908.474		1
1	1	0	16840.429	5.7	2				16913.851	5.7	2	16913.535		1
2	0	2	16862.895	9.4	2				16940.629	9.4	2	16940.235	13.7	2
2	1	2	16873.744		1	16878.026		1	16947.859	8.1	2	16947.579	14.0	2
2	1	1	16890.803	2.0	2				16963.130	4.8	2			
2	2	1	16934.743		1				16997.232	4.1	2	16997.158		1
2	2	0	16935.897	2.6	2	16933.302		1	16998.753	4.2	2	16998.550		1
3	0	3	16924.975	3.9	2	16927.232	9.8	2	17001.077	2.9	2	17000.660	7.2	3
3	1	3	16931.569	9.4	2	16936.017	21.0	2	17006.098	0.0	2	17005.395	6.2	3
3	1	2	16965.318	7.4	2	16971.751	14.2	2	17035.922	3.6	3	17035.598	1.2	3
3	2	2	17001.662	1.7	3	16999.058	7.4	2	17063.768	4.8	3	17063.848		1
3	2	1	17008.435	8.8	3	17005.404	9.9	2	17070.088	7.6	3	17070.022	4.9	3
3	3	1	17083.619	7.0	2	17082.457		1	17138.736	5.9	2	17137.421		1
3	3	0	17083.856	0.3	2	17082.702		1	17138.966	3.9	2	17137.628		1
4	0	4	17004.235	10.8	2	17010.364	2.4	2	17079.356	1.8	2	17079.173	9.4	2
4	1	4	17006.961	2.0	2	17012.284	3.2	3	17081.528	3.4	2	17081.378	5.8	3
4	1	3	17062.430	11.5	2	17071.209		1	17130.655	8.0	3	17130.388	16.6	3
4	2	3	17089.543	3.1	3	17087.030	0.6	2	17151.318	6.1	2	17151.545	8.2	3
4	2	2	17106.187	2.9	3	17103.291	2.2	2	17167.451	6.0	4	17167.557		1
4	3	2	17174.188	2.1	3	17173.159	2.6	2	17230.588	0.3	3	17229.229		1
4	3	1	17175.674	0.2	2	17174.701	19.4	2	17232.052	6.4	3	17230.650		1
4	4	1	17273.011		1	17272.421	2.8	2	17345.023		1	17343.784		1
4	4	0	17273.297	8.3	3	17272.502		1	17344.996		1	17343.786		1
5	0	5	17098.881		1	17102.719		1	17174.909	8.6	2	17173.823	7.6	3
5	1	5	17099.444		1	17105.902		1	17174.993	2.3	2	17173.936	13.2	2
5	1	4	17179.875	1.1	2	17174.210		1	17245.123	1.6	2	17244.972		1
5	2	4	17197.436	3.2	2	17195.067		1	17259.003	6.2	3	17259.530	9.0	2
5	2	3	17229.592	5.6	2	17226.505	12.7	2	17290.418	10.3	3	17290.819	7.6	3
5	3	3	17286.838	9.8	4	17285.892	1.1	2	17345.313	4.3	4	17343.838		1
5	3	2	17292.615	6.3	3	17291.805		1	17351.051	4.2	3	17348.871	8.7	2
5	4	2	17386.151	4.4	2	17385.659		1	17461.631		1			
5	4	1	17386.501	18.3	2	17386.022	6.8	2				17460.559		1
5	5	1	17481.582		1	17481.351		1						
5	5	0	17481.579	0.6	2	17481.324		1						
6	0	6	17210.005		1	17215.015		1	17285.756	9.8	3	17285.087		1
6	1	6				17217.608		1	17285.765	4.6	2	17285.053		1
6	1	5	17315.417	26.7	2	17311.782		1	17377.466	13.0	3	17377.483		1
6	2	5	17324.302		1	17321.993	6.4	3	17385.936	4.8	2	17386.175	6.7	4
6	2	4	17376.552	4.5	3	17373.026		1	17435.707	14.7	2	17436.723		1
6	3	4	17421.752	3.4	3	17420.684	1.3	2	17482.344	0.9	3	17480.675	5.0	2
6	3	3	17434.884	9.9	2	17521.950		1	17494.398	1.5	2	17493.452		1
6	4	3	17523.657		1				17601.601		1	17600.387		1
6	4	2	17524.307	5.6	2	17523.413		1						
6	5	2	17617.891	5.4	2	17617.681		1	17773.448		1			
6	5	1	17617.906	8.9	3	17617.775		1	17773.452		1			
6	6	1	17750.873		1	17745.243		1						
6	6	0	17750.873		1	17745.239		1						
7	0	7	17328.143		1	17343.962		1	17412.671	1.6	2			
7	1	7				17345.830		1	17413.344	5.7	3	17413.039		1
7	1	6	17466.893		1							17527.176		1
7	2	6	17469.558	6.2	2				17531.411		1	17533.271		1
7	2	5	17544.033	0.7	2	17539.962		1	17610.338		1	17609.082	3.1	2
7	3	5	17576.927	16.3	2	17575.992		1	17640.767		1	17638.869		1
7	3	4	17606.965		1	17606.418		1	17666.841		1	17664.428		1
7	4	4	17680.687		1	17679.648		1	17765.072		1			
7	4	3	17685.263	11.9	2	17686.703		1						
7	5	3				17776.715		1						
7	5	2				17777.023		1						
7	6	2	17908.538	14.9	2	17903.357		1						
7	6	1	17908.536	17.7	2	17903.321		1						
7	7	1				18054.558		1						

Table 2 (*continued*)

J	K_a	K_c	(321)		(420)		(401)		(500)	
7	7	0			18054.558	1				
8	0	8	17480.218	1	17489.375	1	17557.813	1	17557.151	1
8	1	8			17495.650	1	17557.769	1	17557.548	1
8	1	7	17629.496	1			17693.568	1		
8	2	7	17614.643	1					17700.215	1
8	2	6	17729.099	1			17786.345	1		
8	3	6			17750.816	1			17817.599	1
8	3	5	17800.129	1	17798.843	1	17859.471	1		
8	4	4	17873.015	1	17871.827	1	17960.256	1		
8	5	4			17957.879	1				
8	5	3	17959.150	1						
8	6	3			18083.555	1				
8	6	2			18083.623	1				
8	7	2			18233.506	1				
8	7	1			18233.501	1				
9	0	9					17719.223	1		
9	1	9					17717.897	1		
9	1	8							17881.549	1
9	2	8	17803.428	1						
9	2	7	17944.381	1						
9	3	7					18020.385	1		
9	3	6		1	18013.991	1				
9	4	6			18061.642	1	18166.120	1		
10	0	10	17808.943	1			17897.202	1		
10	1	10	17811.656	1						
10	2	9	18002.266	1					18069.909	1
10	5	5	18396.659	1						

Also given are the root mean square experimental uncertainties in 10^{-3} cm^{-1} for energy levels derived from two and more lines and the number of transitions used in the level derivation.

underestimate of the line strength in typical pulsed CRD experiments, caused by multi-exponential contributions to the decays for situations where the laser line width approaches the widths of the resonances [10]. For the weak lines, as well as for blended lines, the uncertainty may reach 100–300%, an estimate based on the tendency of (obs. − calc.)/obs. in the intensities, and on the known quality of the SP dipole moment surface [14]. For the strongest lines the experimental values seem to be greatly underestimated due to saturation effects in the CRD experiments.

Comparisons of line positions and intensities were used to suggest possible assignments; additional ingredients for achieving reliable line assignments are combination differences, as well as ratios of new energy levels of $H_2{}^{17}O$ to known levels of $H_2{}^{16}O$ and $H_2{}^{18}O$. Identification of the four strongest bands formed by transitions involving rotational sublevels of two local mode pairs: (321)–(420) and (401)–(500) was facilitated by the use of the fact that the rotational structure of the components of local mode pair has to be identical. The assignment procedures have led to positive identification of all 516 lines attributed to $H_2{}^{17}O$. All the transitions originate in the (000) vibrational ground level and are assigned to 14 different upper levels including (321), (420), (500), and (401). A summary of vibrational energy levels included in the present analysis is given in Table 1.

Fig. 2 shows a comparison of the experimental spectrum with the calculated line list. Of the 516 observed lines, the 65 strongest ones were excluded from the comparison since their intensities were greatly underestimated due to saturation. The assignment of the strongest lines is not so difficult, even if they are saturated: as usual, they correspond to transitions involving low J values, and are part of well-behaved combination differences (CD). The main problem is assignment of medium intensity and, especially, the weakest lines, which often are not included into CD relations. As it is seen from the figure, observed and calculated intensities agree well throughout the entire range, confirming a high accuracy of the calculated data and the assignments performed. In the resulting identification list, the calculated intensities are presented along with the observed values. For the strongest observed lines, corresponding to calculated intensities larger than 2.2×10^{-28} cm molecule^{-1} (natural abundance), the calculated data are more precise, in view of the saturation in the experimental data.

The band origins for (321) and (401) are newly determined at 16797.167 and 16875.620 cm^{-1}, respectively. For (500) and (420) band origins were not directly observed experimentally, thus they are estimated at 16875.27 ± 0.02 and 16798.83 ± 0.1 cm^{-1}, respectively from the obs. − calc. tendency for the energy levels [$J0J$] (in conventional [J, K_a, K_c] notation). The band origin for (500) has not been observed for either $H_2{}^{16}O$ or $H_2{}^{18}O$. The Obs. − Calc. differences were reasonably systematic for energy levels of all four above-mentioned states, while for the other ten states the obs. − calc. ten-

Table 3
$H_2{}^{17}O$ energy levels in cm^{-1} for (340), (260), (302), (142), (222), (123), (043), (241), (161), and (081) vibrational states

(340)					
4	3	2	17003.351	12.3	2
4	4	1	17180.383	11.2	2
4	4	0	17180.333		1
5	3	2	17120.958		1
5	4	2	17297.767	0.7	2
6	4	3	17439.310	5.4	2
6	5	2	17663.621		1
6	5	1	17663.654		1
7	3	5	17421.573		1
7	3	4	17430.236		1
7	4	4	17599.878		1
7	5	3	17827.467		1
7	5	2	17827.712		1
9	2	7	17725.894		1
(241)					
4	3	2	17004.696	6.0	2
4	4	1	17182.849		1
4	4	0	17182.822		1
5	4	2	17300.006		1
5	5	0	17523.875		1
6	3	3	17270.407		1
6	4	3	17440.738	26.2	2
6	4	2	17442.315	20.2	2
7	4	4	17601.678		1
(302)					
4	4	1	17862.098		1
4	4	0	17862.094		1
(123)					
6	0	6	17701.228		1
6	1	5	17809.266		1
(222)					
4	1	4	17414.118		1
(142)					
3	0	3	16901.708		1
3	1	2	16954.765		1
4	1	4	16993.400		1
4	2	3	17128.444	6.8	2
4	3	2	17272.364		1
5	0	5	17082.689		1
5	1	5	17087.879		1
5	1	4	17193.189		1
5	2	3	17267.082		1
6	1	6	17199.139		1
6	2	5	17367.961		1
7	2	5	17594.981		1
8	1	8	17478.691		1
8	2	7	17684.477		1
9	0	9	17652.142		1
9	1	9	17649.025		1
9	1	9	17649.025		1
(043)					
3	0	3	17068.650	0.1	2
3	1	3	17081.924		1
5	1	4	17349.543	2.6	3
5	3	3	17522.873		1
6	1	5	17496.478	14.7	3
(260)					
6	5	2	17521.583	2.0	2
6	5	1	17520.658		1
7	5	3	17683.552		1
(161)					
6	4	2	17215.931		1
(081)					
8	5	3	17691.982		1

The three quantum numbers preceding the level energies are J, K_a and K_c. Also given are the root mean square experimental uncertainties in 10^{-3} cm^{-1} for energy levels derived from two and more lines and the number of transitions used in the level derivation.

dencies were less obvious since only separate energy levels were derived for these states from the perturbed transitions borrowing their intensity from stronger bands. The level energies for all considered states are tabulated in Tables 2 and 3. The averaged absolute deviation between level energies as derived from experiment and from calculation is 0.08 cm^{-1}, whereas the maximal deviation is -0.33 cm^{-1}. These values represent the criteria on the accuracy of the theoretical models. As the presently observed levels were not included in the fitting procedure in [13] the standard deviation shows good extrapolation quality of the PES used for generating theoretical line list.

4. Discussion and conclusion

Fewer lines were attributed to $H_2{}^{17}O$ in this spectrum compared to the $H_2{}^{18}O$ lines in the same spectral region [5]. This is because the sample used in this experiment contained a lower concentration of $H_2{}^{17}O$ and also the spectrum was significantly contaminated by $H_2{}^{16}O$ and $H_2{}^{18}O$. We decided to keep all the $H_2{}^{17}O$ lines overlapped by lines pertaining to other isotope species in the line list, if the contribution from the $H_2{}^{17}O$ was more than 30–50%. However, some relatively strong predicted $H_2{}^{17}O$ lines were not found in the spectrum since the corresponding experimental lines were unrecoverably blended by near-by much stronger $H_2{}^{16}O$, $H_2{}^{18}O$, or other $H_2{}^{17}O$ lines. For the strongest vibrational level in the considered polyad region, the (401) vibrational mode, many energy levels are confirmed by combination differences. However, for the less strong modes like (321), (500), and others, energy levels were determined from a single transition (60% in total). The energy levels determined by a single weak transition are less reliable than those confirmed by combination differences.

Many energy levels of the highly excited states like (340), (142), and (241) (see Table 3) were derived from the transitions borrowing intensity from resonance partners belonging to the four strongest bands. To perform reasonable rovibrational labelling of these highly excited levels was rather difficult. As it was mentioned above, the ratios of

new energy levels of $H_2{}^{17}O$ to known levels of $H_2{}^{16}O$ and $H_2{}^{18}O$ were used not only for assignment, but for labelling purposes also. However, a number of newly observed $H_2{}^{17}O$ energy levels were not available for the $H_2{}^{16}O$ and $H_2{}^{18}O$ molecules. In this case, the labelling was determined on the basis of calculations within the effective Hamiltonian approach.

As it was anticipated, the line intensities generated using the DMS of [14] and the PES of [13] were found to be, on average, very close to those obtained with the same DMS of [14] and the PES by Partridge and Schwenke [16]. However, in some cases, these intensities differed strongly, in particular for transitions involving upper energy levels in close (less than 1 cm^{-1}) resonance. Thus, the SP intensities for transitions (500)[717]–[808] at 16670.641 cm^{-1}, and (500)[717]–[606] at 16967.364 cm^{-1} were predicted to be 6.6×10^{-30} and 2.0×10^{-30} cm molecule^{-1}, respectively, while the experimental values were of 2.27×10^{-29} and 4.55×10^{-29} cm molecule^{-1}, close to the ones evaluated in [13,14]: 2.3×10^{-29} and 3.9×10^{-29} cm molecule^{-1}. Better agreement of the latter intensities with the observed values is a result of using more correct wave functions as provided by [13].

The $H_2{}^{17}O$ water vapor spectrum in the 5ν polyad measured by CRD spectroscopy has been analysed and all 516 observed lines are now assigned yielding an important number of 303 new highly excited energy levels. The complete assignment of the observed $H_2{}^{17}O$ lines has been made possible due to high-quality synthetic spectrum provided by [13,14], while the well-known calculation by Schwenke and Partridge [14,16] may be inaccurate in the considered spectral range up to 5 cm^{-1}. This is the highest frequency region to be studied for $H_2{}^{17}O$, and as such it adds to the understanding of the entire water spectrum.

Acknowledgments

The authors acknowlegde the contribution by N.F. Zobov and O.L. Polyansky (Nizhnii Novgorod) to the generation of the line list for $H_2{}^{17}O$, that will be published independently [13]. This research forms part of an effort by a Task Group of the International Union of Pure and Applied Chemistry (IUPAC, Project No. 2004-035-1-100) on 'A database of water transitions from experiment and theory.' This work is supported by the Space Research Organization Netherlands (SRON) with a Project Grant (EO 036), and by the European Community—Access to Research Infrastructures action of the Improving Human Potential program, Contract No. HPRI–CT–1999–00064, as well as the INTAS foundation and the Russian Foundation for Basic Research.

Appendix A. Supplementary data

Supplementary data for this article are available on ScienceDirect (www.sciencedirect.com) and as part of the Ohio State University Molecular Spectroscopy Archives (http://msa.lib.ohio-state.edu/jmsa_hp.htm).

References

[1] A.N. Maurellis, R. Lang, J.E. Williams, W.J. van der Zande, K. Smith, J. Tennyson, R.N. Tolchenov, The impact of new water vapor spectroscopy on satellite retrievals, NATO SCIENCE series: IV. Earth and Environmental Sciences, 27, Kluwer Academic Publishers, 2003, pp. 259–270.
[2] R. Lang, A.N. Maurellis, W.J. van der Zande, I. Aben, J. Landgraf, W. Ubachs, J. Geophys. Res. 107 (D16) (2002) 4300.
[3] H. Naus, W. Ubachs, P.F. Levelt, O.L. Polyansky, N.F. Zobov, J. Tennyson, J. Mol. Spectrosc. 205 (2001) 117–121.
[4] S. Kassi, P. Macko, O. Naumenko, A. Campargue, Phys. Chem. Chem. Phys. 7 (2006) 2460–2467.
[5] M. Tanaka, M. Sneep, W. Ubachs, J. Tennyson, J. Mol. Spectrosc. 226 (2004) 1–6.
[6] R.A. Toth, J. Opt. Soc. Am. B 9 (1992) 462–482.
[7] R.A. Toth, Appl. Opt. 33 (1994) 4868–4879.
[8] C. Camy-Peyret, J.-M. Flaud, J.-Y. Mandin, A. Bykov, O. Naumenko, L. Sinitsa, B. Voronin, J. Quant. Spectrosc. RA 61 (1999) 795–812.
[9] M. Tanaka, O. Naumenko, J.W. Brault, J. Tennyson, J. Mol. Spectrosc. 234 (2005) 1–9.
[10] H. Naus, I.H.M. van Stokkum, W. Hogervorst, W. Ubachs, Appl. Opt. 40 (2001) 4416–4426.
[11] S. Gerstenkorn, P. Luc, Atlas du Spectroscopie d'Absorption de la Molecule de l'Iode Entre 14800–20000 cm^{-1}, Presses du CNRS, 1978.
[12] J. Tennyson, M.A. Kostin, P. Barletta, G.J. Harris, J. Ramanlal, O.L. Polyansky, N.F. Zobov, Comp. Phys. Commun. 163 (2004) 85–116.
[13] S.V. Shirin, O.L. Polyansky, N.F. Zobov, A.G. Császár, R.I. Ovsyannikov, J. Tennyson, J. Mol. Spectrosc. 236 (2006) 216–223.
[14] D.W. Schwenke, H. Partridge, J. Chem. Phys. 113 (2000) 6592–6597.
[15] L.S. Rothman et al., J. Quant. Spectrosc. RA 96 (2005) 139–204.
[16] H. Partridge, D.W. Schwenke, J. Chem. Phys. 106 (1997) 4618–4639.